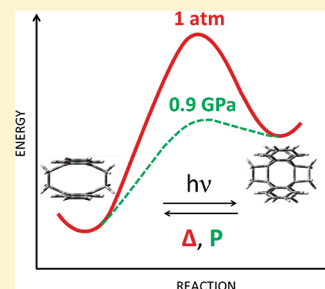


Pressure Catalyzed Bond Dissociation in an Anthracene Cyclophane Photodimer

Sebastian R. Jezowski, Lingyan Zhu, Yaobing Wang, Andrew P. Rice, Gary W. Scott, Christopher J. Bardeen,* and Eric L. Chronister*

Department of Chemistry, University of California, Riverside, California 92521, United States

ABSTRACT: The anthracene cyclophane bis-anthracene (BA) can undergo a [4 + 4] photocycloaddition reaction that results in a photodimer with two cyclobutane rings. We find that the subsequent dissociation of the dimer, which involves the rupture of two carbon–carbon bonds, is strongly accelerated by the application of mild pressures. The reaction kinetics of the dimer dissociation in a Zeonex (polycycloolefin) polymer matrix were measured at various pressures and temperatures. Biexponential reaction kinetics were observed for all pressures, consistent with the presence of two different isomers of bis(anthracene). One of the rates showed a strong dependence on pressure, yielding a negative activation volume for the dissociation reaction of $\Delta V^\ddagger = -16 \text{ \AA}^3$. The 93 kJ/mol activation energy for the dissociation reaction at ambient pressure is lowered by more than an order of magnitude from 93 to 7 kJ/mol with the application of modest pressure (0.9 GPa). Both observations are consistent with a transition state that is stabilized at higher pressures, and a mechanism for this is proposed in terms of a two-step process where a flattening of the anthracene rings precedes rupture of the cyclobutane rings. The ability to catalyze covalent bond breakage in isolated small molecules using compressive forces may present opportunities for the development of materials that can be activated by acoustic shock or stress.

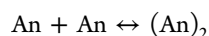


1. INTRODUCTION

The field of mechanochemistry concerns the application of mechanical force to induce the breaking and formation of covalent chemical bonds.^{1–3} Materials that undergo chemical reactions when subjected to pressure or strain can have a variety of applications as sensors or as components of “self-healing” polymers. The simplest example of the experimental application of mechanical force involves the grinding of crystalline solids and observing the changes in color or chemical composition that result.^{1,2,4–7} Another form of anisotropic force involves applying mechanical tension to the ends of a reactive molecule. For example, the application of well-defined forces to the ends of polymers, often using a scanning probe microscope, can pull bonds apart in a controlled way.^{8–10} A simpler way to generate mechanical force is to use collapsing cavitation bubbles associated with ultrasonic excitation to generate microscopic tension that can activate covalent bond scission in polymers.^{1,11–13} For these tensile forces to effectively couple to reactive units, it is often necessary to covalently incorporate mechanochemical species into polymer chains,^{14,15} which has been shown to accelerate rearrangement reactions and bias reaction products,^{11,16} for example, ultrasound-induced electrolytic ring-opening reactions for 1,2-disubstituted benzocyclobutene.¹¹ Interpretation of these experiments can be complicated by the fact that the mechanical action of ultrasound is accompanied by thermal effects.¹³ A common theme of this area of research has been the design of molecules that are uniquely sensitive to the application of directional forces.¹⁷ This directionality has often been obtained by utilizing covalent bonding to polymers

that transmit tensile or shear forces to mechanophores that otherwise would have been largely inert to mechanical force.^{5,18}

Rather than applying directional stress, as in the scanning probe experiments and sonochemical studies of covalent polymer systems, the present study concerns the application of isotropic compressive force as a means of inducing mechanochemical bond cleavage for isolated small molecules in solid solution. More than 35 years ago, Drickamer and co-workers demonstrated that bianthrone and spiropyran chromophores doped into polymers could undergo a pressure-induced reaction to their colored forms.^{19,20} The lower volumes of the products favored their equilibrium concentrations at high pressures. Since then, several instances of cis–trans isomerizations driven by pressure have been reported,^{21,22} but in general, the pressures required for bond breaking have resided in the range of 10–20 GPa,^{23–25} well above the stresses needed to mechanically fracture molecular solids. In analogy with the work described above, it would be desirable to design a molecule that is more sensitive to pressure changes. In this paper, we use photochemistry to make a highly strained molecule²⁶ that undergoes accelerated bond dissociation below 1 GPa pressure. The pressure-catalyzed bond breaking relies on reversion of the anthracene (An) [4 + 4] photodimerization reaction:



Received: January 13, 2012

Published: April 9, 2012



This well-known reaction has potential uses for both information²⁷ and energy storage²⁸ and has also demonstrated interesting photomechanical properties.^{29–33} The forward reaction is driven by the absorption of high energy photons, while the dissociation into monomers is typically accomplished by heating or by absorption of higher energy photons. The photodimerization reaction is robust and occurs for a wide range of modified anthracene monomers.^{28,34,35} For polyacene molecules embedded in a crystal or polymer, the dimerization reaction depends on both their orientation and the distance between the two anthracene moieties. As observed in many dimerization reactions, higher pressures decrease the intermolecular distance and favor dimer formation while suppressing their dissociation back into monomers³⁶ at the same time. The bianthracene cyclophane molecule that is the subject of this paper shows the opposite behavior: the rate of dissociation is strongly enhanced by applying mild pressures. In bi-(anthracene-9,10-dimethylene) (BA), the anthracene moieties are tethered together in a favorable face-to-face topological orientation for photoreaction. The reaction sequence is outlined in Figure 1, which shows the structure of BA

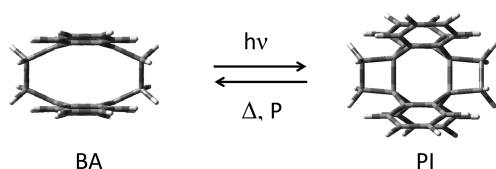


Figure 1. Absorption of visible light by bis-anthracene (BA) leads to the formation of a photoisomer (PI) characterized by the formation of two additional covalent bands between the linked sandwich anthracene moieties. The reverse reaction can be accelerated with heat and, as demonstrated in this paper, with the application of pressure.

interconverting between its monomeric and dimeric photoisomer (PI) form. When the metastable photodimer is created in a polymer matrix, it is stable for days, very slowly converting back to its monomeric form. When moderate ~ 1 GPa pressures is applied, the dimer dissociation back into a pair of tethered monomers is greatly accelerated, and above 1.5 GPa, the dissociation occurs within seconds. The regular $[4 + 4]$ anthracene photodimer (An_2) is stable under the same conditions and shows no pressure enhancement of the dissociation rate. Various methods indicate that the molecular volumes of BA and PI are the same to within 1% or less, so there is no indication that pressure should favor either the reactant or the product. Pressure- and temperature-dependent kinetic measurements indicate a negative activation volume and a reduced activation barrier at high pressure, suggesting that high pressure stabilizes the transition state of the dissociation reaction. These facts suggest a novel mechanism for the pressure-induced chemical reaction: that the strained dimer distorts in a specific way that transiently lowers the total volume as it evolves to the lowest energy (dissociated) state. In this case, pressure provides a kinetic acceleration of the reaction of the metastable PI dimer, rather than changing the relative thermodynamic stability of the reactant or product. This work demonstrates a counterintuitive chemical reaction where a molecule undergoes mechanically accelerated bond breaking under relatively mild conditions. The ability to catalyze covalent bond breakage in isolated (i.e., noncovalently bound) molecules using compressive forces may present opportunities

for the development of materials activated by acoustic shock or stress.

2. EXPERIMENTAL SECTION

2.1. Sample Preparation. Crystalline bi-(anthracene-9,10-dimethylene) (BA) was synthesized from 9,10-di(chloromethyl)-anthracene (TCI America) and purified in the dark as originally described.³⁷ Chemicals were purchased commercially and used without further purification.

Spectroscopic investigations of BA, PI, An, and An_2 were performed as dilute solutes in polymer films. BA was blended into UV-transparent (>237 nm) polycycloolefin resin (ZEONEX Z480, $T_g = 138–140$ °C, Zeon Chemicals L.P.). Yellow crystals of BA and colorless pellets of Zeonex polymer were codissolved in a few milliliters of cyclohexane (EMD ACS grade). The mixture was ultrasonicated in the dark for about 2 h, after which the solvent was allowed to evaporate in the air at room temperature and in the dark. Transparent yellowish films of BA-doped Zeonex films were obtained (~ 0.24 mm thick, $\sim 0.5\%$ BA by weight) and used in pressure- and temperature-dependent studies. Dilute polymer films of BA were utilized to obtain a convenient optical density for spectroscopic studies, and the polymer matrix provided a reasonably hydrostatic pressure medium under the pressure range of this study, as discussed in the next section. The Zeonex polymer was chosen for its UV transparency needed to resolve the major BA absorption band near 260 nm. Studies have shown that intramolecular chemistry and photophysics can be largely insensitive to different particular polymer systems.³⁸

Zeonex films containing BA were sealed in an airtight cell to protect against oxidation and heated to ~ 50 °C in the dark for a period of about 2 h to remove any PI that may have formed during synthesis. No evidence of pressure-induced chemical changes in either the BA or the Zeonex matrix was observed up to 7.2 GPa. The BA absorption spectrum showed a pressure-dependent shift of $450\text{ cm}^{-1}/\text{GPa}$ consistent with the increased density and polarizability of the polymer matrix under pressure. Above 1.5 GPa, the pressure shift decreases significantly due to reduced compressibility of the matrix. Controls were performed to confirm the absence of pressure- or light-induced degradation in pure Zeonex induced by either temperature (up to 80 °C) or mechanical stress (up to 7.2 GPa). Samples intentionally exposed to air showed some absorption anomalies after heating above 50 °C, which we attribute to oxidation of the Zeonex film.

2.2. Photophysical Measurements at Variable Temperature and Pressure. Temperature- and pressure-dependent measurements were performed by placing the BA sample film in a diamond anvil cell (DAC). The DAC utilized type II diamonds (with 0.5 mm culet diameter) with an inconel gasket, and a typical sample size was $\sim 400\text{ }\mu\text{m}$ in diameter and $\sim 100\text{ }\mu\text{m}$ thick. A small amount of ruby was added to the sample, and the ruby emission was used to determine the pressure of the sample with an accuracy ± 0.5 kbar. The BA absorption band near 260 nm showed a red shift of $450\text{ cm}^{-1}/\text{GPa}$ under pressure, which provided a sensitive internal pressure standard. Pressure broadening in the BA absorption band was not observed below 2 GPa, indicating that the underlying pressure inhomogeneity was small relative to the applied pressure. Pressure broadening of 5–10% was observed in the ruby emission spectrum but even at this level would not be a limiting factor in the analysis of the pressure-dependent reaction kinetics. Temperature-dependent measurements utilized resistive heating of the DAC, and the temperature was monitored using a thermocouple (type K, Omega HH22) in contact with the DAC.

UV–vis absorption spectra were obtained using a Varian CARY 500 spectrometer (0.5 nm/step with 0.2 s integration time). Two 38 mm focal length lenses (SI–UV grade) were utilized to focus the transmitted light through the $\sim 400\text{ }\mu\text{m}$ diameter DAC sample aperture. The spectra were referenced to the absorption of a pure Zeonex film loaded in the same DAC at 1 atm pressure and room temperature. The spectrometer excitation intensity was orders of magnitude weaker than the photolysis source, and control experiments confirmed that negligible photochemistry was induced during the

spectrometer scans. The photoconversion and reversion reactions were quantified by the changes in the integrated area of the major BA absorption band (~ 257 nm at 1 atm). The absorption red shift associated with increased pressure was taken into account in the spectral analysis.

To initiate the BA \rightarrow PI photochemical reaction, a halogen lamp was used as the source of visible light. The excitation light was passed through a 1 cm thick water filter to reduce IR heating, and wavelengths below 300 nm were blocked by the glass optics. The visible light irradiance at the sample was ~ 120 mW/cm². To measure the kinetics of the PI \rightarrow BA reaction, a photoconverted polymer sample was placed in a DAC, and the three connecting bolts were tightened to generate a pressure “jump” within 30 s. The ensuing absorption scans of the UV region of the PI absorption spectrum required ~ 30 s as well, which determines the overall time resolution of the system. The resulting pressure was measured after the experiment by the ruby emission shift and the intrinsic red shift of the BA absorption band.

2.3. Computational Modeling. Quantum calculations were utilized to determine the structures and heats of formation of both BA and PI. Calculations were carried out using the Kohn–Shan density functional theory including dispersion (DFT-D),³⁹ employing a 6-31+G(d) basis set to allow determination of most accurate thermodynamic information for molecules of the size of BA. The dispersion-improved forcefield includes semiempirically corrected noncovalent interactions, which can be significant for aromatic sandwich dimer molecules such as BA. The molecular volumes contained inside of a 0.001 electrons/Bohr³ density contour were estimated using Monte Carlo integration, with the use of 10000 integration points.⁴⁰ Each integration was repeated 100 times, and the resulting standard deviation for the calculated volumes was less than 0.5%. All calculations were performed using the multiprocessor version of Gaussian 09W.

3. RESULTS

3.1. Light-Induced Cycloaddition of Tethered BA \rightarrow PI. At ambient temperature and pressure conditions, BA shows a major absorption band around 257 nm, a weaker shoulder band at around 280 nm, and a broad absorption band from ~ 350 to ~ 450 nm, as shown in Figure 2. Excitation in the ~ 350 – 450 nm band initiates a $[4 + 4]$ cycloaddition reaction

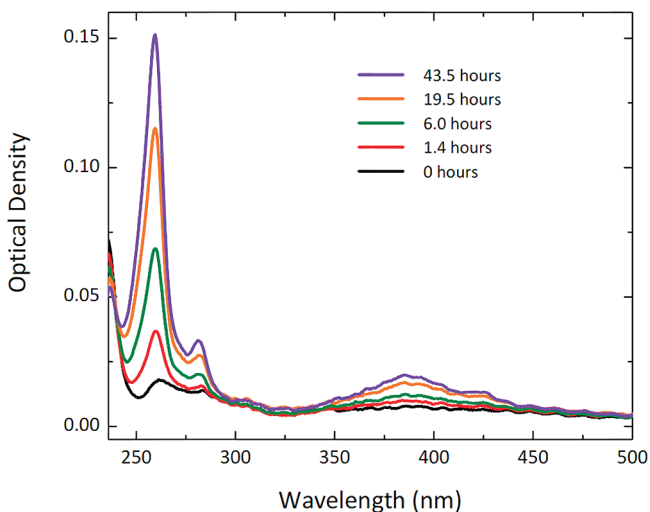


Figure 2. Time-dependent spectral evolution of PI at a pressure of 0.6 GPa. The black trace is the absorption spectrum of photochemically generated PI immediately after excitation and just before the application of pressure. The increased pressure accelerates the rate of conversion of PI (lower, black) \rightarrow BA (top, purple). The spectral changes were followed until an absorption spectrum characteristic of unphotolyzed BA (top, purple) was obtained.

(BA \rightarrow PI) that proceeds through the excited electronic state. Visible illumination irradiance of ~ 120 mW/cm² (only ~ 10 mW of which lies in the 350–450 nm range) resulted in nearly complete photoconversion of BA \rightarrow PI in ~ 20 s at ambient pressure. Longer illumination times were required at elevated pressures to achieve the same level of photo conversion; for example, at ~ 0.9 GPa, roughly 3 \times more excitation fluence was required for photoconversion relative to ambient pressure. At pressures ≥ 2.0 GPa, light-induced formation of PI was almost entirely inhibited under the above specified irradiation conditions.

In the intramolecular photoisomer (PI) product, the extended conjugation of the anthracene moieties is lost. Spectroscopically, this is confirmed by a reduction in the major BA absorption bands characteristic of anthracene, for example, the main band ~ 257 nm and the anthracene bands between ~ 325 and 450 nm. The cycloaddition reaction yields a PI product with a much weaker absorption band near ~ 262 nm, attributed to the B-band of the four mutually bound ortho-substituted benzene chromophores in PI,⁴¹ which is several orders of magnitude lower than the extinction coefficient of the main BA absorption band. The higher energy UV absorption bands associated with the substituted benzene chromophores in PI overlap with the UV absorption of the Zeonex polymer and are not displayed. In this study, the major BA absorption band centered at ~ 257 nm was used as a spectroscopic marker for quantifying the extent of photoconversion as well as thermally or mechanically induced covalent bond cleavage associated with the PI \rightarrow BA dissociation back-reaction.

3.2. Dissociation of PI \rightarrow BA. Untethered An₂ is thermally stable up to 200 °C⁴² (with a dissociation energy barrier of 155 kJ/mol⁴³). In contrast, the tethered PI photoisomer is known to slowly dissociate into BA under ambient pressure and temperature conditions in solution^{37,42} and in its crystalline form.⁴⁴ PI dissolved in toluene shows simple first-order kinetics for the thermally activated PI \rightarrow BA reaction, with an activation energy of 100.4 kJ/mol.⁴² In the pure solid, the PI \rightarrow BA back-reaction displays more complex biexponential kinetics,⁴² which has been attributed to a bimolecular BA-catalyzed conversion of PI \rightarrow BA.⁴²

In agreement with previous reports, we find that the relatively low potential energy barrier for the PI \rightarrow BA back-conversion²⁸ yields nearly complete reversion of PI to BA in Zeonex within weeks under ambient conditions. The rate of PI \rightarrow BA conversion in a dilute mixture is only mildly dependent on the surrounding matrix.⁴² The average rate constant for PI in Zeonex at ambient temperature and pressure, shown in Table 1, is only a factor of 2 faster than the rate reported for PI in toluene and comparable to the rate reported for PI as a dilute impurity in a host BA crystal.⁴² Interestingly, the rate can be slowed dramatically by a factor of $\sim 30\times$ in crystalline PI, for which steric effects impose an energy barrier that is 5–9 kJ/mol higher than in solution.⁴² In the following sections, we will demonstrate that hydrostatic compression of PI can lead to a lowering of the energy barrier, with a corresponding *enhancement* in the rate of the exothermic PI \rightarrow BA conversion reaction.

The stability of the PI photodimer decreases significantly when subjected to a modest pressure increase. Figure 2 illustrates spectroscopic changes associated with the conversion of PI \rightarrow BA under pressure. The anthracene absorption features at 257 and 375 nm both increase over time, indicating that the PI is dissociating into the more highly conjugated anthracenes

Table 1. Pressure Dependence of the k_1 Rate Constant for the PI \rightarrow BA Conversion Was Obtained by Fitting Kinetic Data (e.g., Fig 3) to the Biexponential eq 1^a

pressure (GPa)	k_1 (min ⁻¹)
0	0.0003
0.62	0.0012
0.71	0.0089
0.85	0.0053
0.93	0.0343
1.12	0.0142
1.40	0.0604
1.95	0.0788
2.56	0.1035

^aThe k_2 rate constant was pressure independent with a value of $k_2 = 0.0012 \text{ min}^{-1}$. The weighting of the two different rates was equal, $X_1 = X_2 = 0.5$.

present in BA. Because of its higher signal-to-noise ratio, the integrated area under the absorption band at 257 nm was used to measure the time-dependent change in BA concentration. The benign absorption red shift ($450 \text{ cm}^{-1}/\text{GPa}$) associated with increased pressure was taken into account in the spectral analysis. The dramatic increase in the rate of the PI \rightarrow BA reaction observed under compression of the PI photoisomer is shown in Figure 3 for three representative pressures. The time

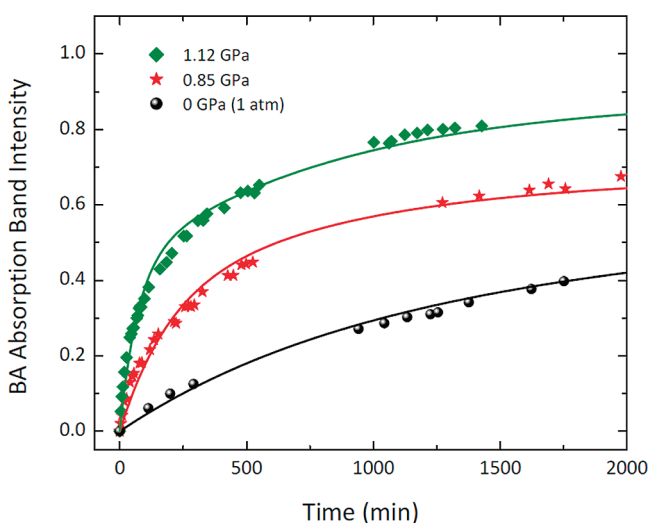


Figure 3. Pressure-enhanced PI \rightarrow BA kinetics at ambient temperature. The rate of formation of BA is found to be enhanced by the application of mechanical compression. The solid curves are biexponential fits to eq 1. The pressure-dependent kinetic rate constants, k_1 , for all nine pressures studied are listed in Table 1.

dependence of the BA absorption band intensity is fit reasonably well with a biexponential:

$$\text{BA}(t) = X_1(1 - e^{-k_1 t}) + X_2(1 - e^{-k_2 t}) \quad (1)$$

where $\text{BA}(t)$ corresponds to the time-dependent normalized area of the main absorption band, k_1 and k_2 are rate constants, and X_1 and X_2 are the relative weighting fractions. The solid curves in Figure 3 are fits to eq 1 using one pressure-dependent constant (k_1), one fixed pressure-independent constant (k_2), and equal weighting $X_1 = X_2 = 0.5$. Reasonable one parameter biexponential fits of the pressure-dependent kinetics were obtained with these constraints, as shown for three

representative pressures in Figure 3. The pressure-independent rate k_2 was fixed at 0.0012 min^{-1} , while the pressure-dependent rate constant k_1 ranged from 0.0003 min^{-1} at ambient pressure to 0.104 min^{-1} at 2.6 GPa. The kinetics of the PI \rightarrow BA reaction in Zeonex was monitored at nine different pressures from ambient to 2.6 GPa, the results of which are summarized in Table 1. The pressure-dependent rate constant, k_1 , increased by more than 2 orders of magnitude at the highest pressure of 2.6 GPa, with most of this change occurring by 1.4 GPa. The dramatic pressure dependence of k_1 adequately models the rapid increase in the rate of the PI \rightarrow BA reaction at high pressure illustrated in Figure 3.

The biexponential kinetics imply the existence of two different populations of PI, one that is sensitive to pressure and reacts with rate k_1 , and one that is insensitive to pressure, corresponding to k_2 . The biexponential kinetics reported for the reconversion of crystalline PI \rightarrow BA have been attributed to a competition between unimolecular dissociation and a bimolecular process in which surrounding BA molecules catalyze the conversion of PI \rightarrow BA.⁴² This mechanism is not relevant to the present study of the dissociation of isolated PI molecules in a polymer matrix. However, computational work has suggested the existence of distinct structural conformers.⁴⁵ The two conformers of BA⁴⁵ involve twisting about the dimethylene bridges to minimize steric repulsions associated with an eclipsed conformation. The less-strained conformer consists of anthracenes rotated with respect to each other about the axis normal to the anthracenes, yielding D_2 symmetry. In the more strained conformer, the anthracenes are translated relative to each other along the long axis of the anthracene, yielding C_{2h} symmetry.⁴⁵ Experimental support for the existence of different conformers is derived from the fact that two crystalline forms of BA have also been identified, α and β .³⁷ The more strained β form has one anthracene translationally displaced from the other, with an increased out of plane dihedral butterfly angle relative to the α form,⁴⁶ similar to the strained conformer identified by the computational work. In crystalline PI, the anthracenes are rotated relative to each other as in the less strained BA conformer, but it is possible that the dissociation reaction can produce either conformer, depending on the local environment. While we have not established the definite presence of different conformations in our experiments, their likely presence provides a reasonable explanation for the multiexponential dissociation kinetics observed at high pressure.

3.3. Activation Energy for the Dissociation of PI \rightarrow BA in Zeonex. To gain insight into the mechanism of the pressure-induced dissociation, we characterized its thermodynamic parameters. Temperature-dependent reaction kinetics yield a measure of the activation energy for the PI \rightarrow BA reaction, illustrated by the Arrhenius plots in Figure 4. The activation energy at ambient pressure was found to be $\Delta E^\ddagger = 93 \text{ kJ/mol}$, consistent with previous measurements at ambient pressure.^{37,42} However, at a relatively modest pressure of 0.9 GPa, the activation energy was reduced by over an order of magnitude, from $\Delta E^\ddagger = 93 \text{ kJ/mol}$ at ambient pressure to only 7 kJ/mol at 0.9 GPa, as shown in Figure 4.

The activation energy of 93 kJ/mol at ambient pressure is considerably less than the energy needed to break a typical chemical bond and is far less than the 155 kJ/mol activation energy reported for the untethered $\text{An}_2 \rightarrow 2\text{An}$ dissociation reaction in benzene.⁴³ Furthermore, our temperature-dependent measurements on An_2 dispersed in Zeonex did not show

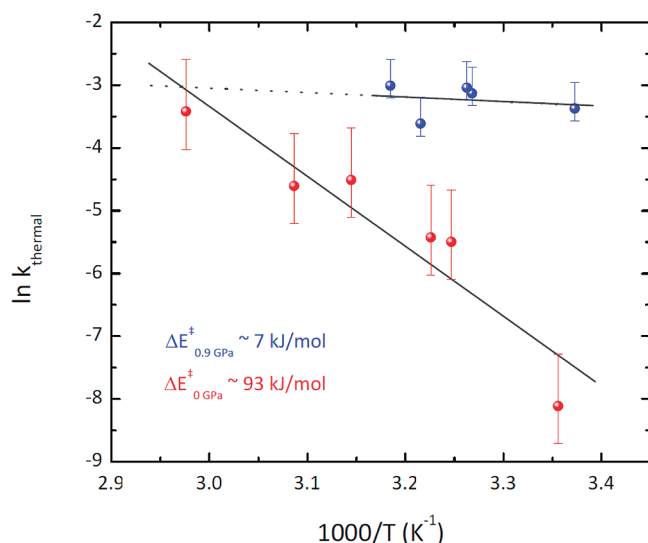


Figure 4. Arrhenius plots for the thermally activated dissociation reaction $\text{PI} \rightarrow \text{BA}$. The activation energy is found to be reduced by over an order of magnitude at 0.9 GPa (blue) vs ambient pressure.

any significant chemical changes up to 80 °C, over a period of 24 h at ambient pressure. This result is consistent with studies of crystalline An_2 ,⁴² for which thermal dissociation only occurs near the melting point. It is interesting that the pressure-dependent kinetic behavior of PI is completely different from that of An_2 . The dimethyl linkers present in PI not only position the anthracene groups for the dimerization but also destabilize the resulting photoisomer, possibly due to the formation of strained cyclobutane rings. The dramatically lowered activation energy at modest pressure suggests that intermolecular interactions are effectively coupled to the reaction coordinate, which involves both releasing strain in the cyclobutane rings and flattening the butterfly angle of the anthracenes (Table 2).

3.4. Activation Volume for the Dissociation of PI → BA. The activation volume can be used as a tool for elucidating reaction mechanisms.⁴⁷ The rate of covalent bond cleavage associated with the $\text{PI} \rightarrow \text{BA}$ reaction is significantly enhanced for pressure increases up to 1.4 GPa, above which the proportional changes in the rate are less pronounced. The rates of the mechanically activated covalent bond-breaking reaction of PI listed in Table 1 can be used to estimate the activation volume (ΔV^\ddagger) for the $\text{PI} \rightarrow \text{BA}$ reaction using the relation:⁴⁷

$$\left(\frac{\partial \ln k_{\text{rxn}}}{\partial P} \right)_T = \frac{-\Delta V^\ddagger}{RT} \quad (2)$$

A plot of the natural log of the k_1 rate constant versus pressure is presented in Figure 5. A negative activation volume of $\Delta V^\ddagger = -16 \text{ \AA}^3$ is obtained by fitting the data in the low-pressure limit

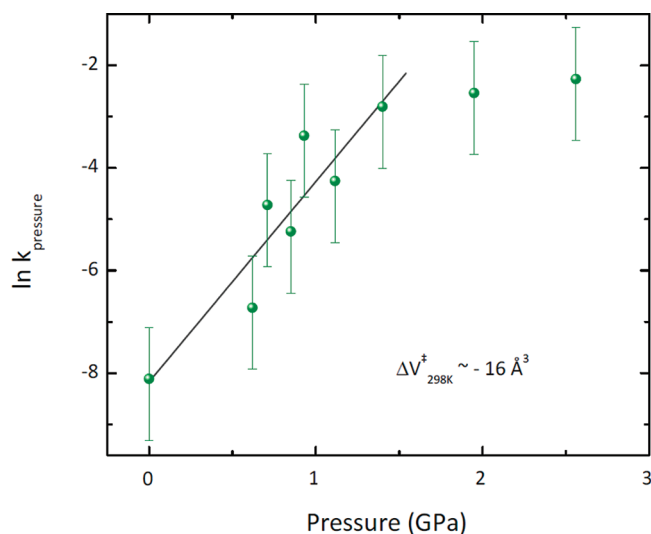


Figure 5. Linear dependence of the log of the rate constant vs pressure up to 1.4 GPa yields an estimate of the activation volume, $\Delta V^\ddagger = -16 \text{ \AA}^3$, for the covalent bond-breaking process in the $\text{PI} \rightarrow \text{BA}$ reaction.

to eq 2. Within a limited pressure range, ΔV^\ddagger can be considered constant,⁴⁷ but above 1.5 GPa, the activation volume becomes negligible, possibly due to competing stabilization of the photodimer under compression.

3.5. Calculated Energetics and Structural Changes. To gain insight into the chemical origins of PI's increased reactivity at higher pressures, we used ab initio calculations to compare the structure and energetics of BA to its relatively unreactive cousin, An_2 . The photochemical reaction of BA leads to the formation of two bridging bonds between C9–C9' and C10–C10' in the PI photoproduct. The photochemistry is facilitated by the dimethyl linkers that hold these carbons in close proximity. We first examine the geometrical characteristics of these two photodimers. The molecular volumes, C9–C9' and C10–C10' distances, and butterfly angles for PI, BA, and An_2 are listed in Table 2. The length of the covalent C–C bonds formed in PI (165 pm⁴⁸) are much longer than typical C–C covalent bonds (153–156 pm⁴⁸) and are also slightly longer than the bridging C–C bonds in An_2 (162 pm⁴⁹). The strain present in the cyclobutane rings in PI likely contributes to the slightly longer C9–C9' and C10–C10' bonds in PI versus An_2 . Crystallographic and calculated values show the same trends and agree to within ~2%. The loss of conjugation upon dimerization leads to an increased nonplanar “butterfly” angle (e.g., defined here as 180° minus the angle defined by the midpoints of C1–C8, C9–C10, and C4–C5). This angle is 0° when the anthracene ring is perfectly planar and increases as the outer edges of the ring bend away from planarity. Note that the small butterfly angle in undimerized BA is due to steric repulsion of the opposing conjugated anthracene moieties. Comparison of the overall geometries of the two dimers does

Table 2. Calculated and Crystallographic Determination of the Butterfly Angle (Defined in the Text), Molecular Volume, and Interatomic Distances [C(9)–C(9') and C(10)–C(10')] for BA, PI, and Dianthracene (An_2)

	BA		PI		An_2	
	calcd	X-ray ⁴⁸	calcd	X-ray ⁴⁸	calcd	X-ray ⁴⁹
butterfly angle (deg)	17.33	16.51	51.13	32.49	49.75	44.38
C(9)–C(9') distance (pm)	283	276	169	165	164	162
molecular volume (\AA^3)	504.3	510.2	504.5	506.5	453.9	463.6

not reveal obvious clues as to why PI should be more sensitive to pressure.

We have also considered the volumes of the reacted and unreacted species. The molecular volumes of the reactant (PI) and product (BA) species were calculated (DFT-D with $\sim 0.5\%$ error) to be 504.5 \AA^3 for PI and 504.3 \AA^3 for BA. These volumes are the same to within the calculation accuracy. A rough estimate of molecular volume can also be estimated from the molar volumes of neat crystals. PI and BA both crystallize in space group $P2_1/c$, with two molecules per unit cell,⁴⁸ with similar molecular volumes of 506.5 and 510.2 \AA^3 , respectively. A naïve interpretation of these volumes would indicate that PI might be favored at higher pressures. However, the small 0.7% difference between the crystal volumes is less than the 0.8% increase observed for a mixed crystal of BA and PI, which illustrates the dominant role that packing interactions can play in determining crystal volumes.⁴⁸ Packing effects are not relevant to isolated PI molecules dissolved in a solid polymer solution, and all indications are that the molecular volumes of the PI and BA are similar and that any volume difference is much smaller than the -16 \AA^3 activation volume obtained using Figure 5 and eq 2. Thus, the volumes of BA and PI provide no clear reason as to why BA would be favored at higher pressures.

We next considered the energetics of the two molecules. Ab initio calculations of the relative energies of the reactant and product species, along with the experimentally determined activation barriers are sketched in Figure 6. The reduction in

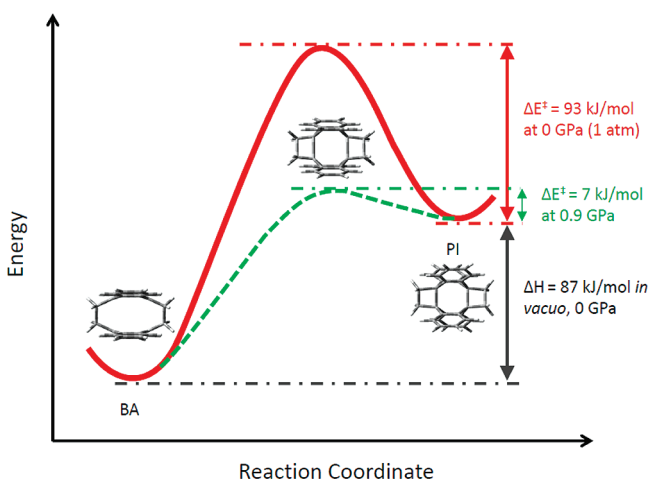


Figure 6. Potential energy diagram for the $\text{BA} \leftrightarrow \text{PI}$ reaction. The difference in enthalpies between the ground states was calculated using dispersion-corrected DFT. The activation energies for the dissociation reaction were determined experimentally at 1 atm and 0.9 GPa (see Figure 4).

the activation barrier at high pressure is also illustrated. Our calculated enthalpy difference between BA and the higher energy PI is 87 kJ/mol . The exothermicity of the $\text{PI} \rightarrow \text{BA}$ reaction has also been confirmed by previous calculations⁴⁵ and calorimetric measurements.^{28,42}

4. DISCUSSION

The results presented in the previous sections show that the photodimerization $\text{BA} \rightarrow \text{PI}$ is inhibited by pressure, while the dissociation $\text{PI} \rightarrow \text{BA}$ is accelerated by pressure. Both results are consistent with destabilization of the PI photoproduct at

higher pressures. We first consider the $\text{BA} \rightarrow \text{PI}$ photoreaction. The ability to accumulate PI depends on both the forward photochemical reaction rate and the reverse dissociation rate. We know that the $\text{PI} \rightarrow \text{BA}$ dissociation rate is enhanced at high pressure, which reduces the amount of PI that can exist at equilibrium under illumination. This effect alone would largely explain our inability to accumulate PI photoproduct at pressures greater than 2 GPa. It is also possible that the photodimerization rate for $\text{BA} \rightarrow \text{PI}$ changes at high pressure, but this rate was not directly measured. Because it does not involve excitation of electronic excited states, we have concentrated on the $\text{PI} \rightarrow \text{BA}$ reaction, and it is this reaction rate that we will proceed to analyze in detail.

It is somewhat surprising that high pressure enhances the $\text{PI} \rightarrow \text{BA}$ dissociation reaction given that: (a) dissociation reactions normally have positive activation volumes⁴⁷ and (b) high pressure has been shown to be effective at stabilizing photodimerized species of polyacene molecules ranging from naphthalene to pentacene.^{36,50} The pressure stabilization of photodimers of untethered polycacenes can be easily understood in terms of their reduced volumes (e.g., the -2.7% volume contraction for An_2 relative to oriented anthracene pairs⁵¹), as well as the entropic effect resulting from the confinement of monomers by the denser, high-pressure medium. When compared to this class of molecules, we can see that both effects are largely absent for BA. Although the light-induced formation of two additional intramolecular covalent bonds might lead one to expect a decrease in the PI molecular volume, the corresponding loss of conjugation in the anthracene moieties leads to an increased bend of the anthracene rings out of planarity. The entropic effect is negated because the dimethyl linkers in BA maintain close contacts between anthracene moieties regardless of the surrounding medium. These two effects oppose each other, as discussed in the previous section, leading to equilibrium molecular volumes that are almost identical. However, a third notable difference between An_2 and PI may help explain their different sensitivities to pressure. When the PI and An_2 volumes are compared, we find that the mass/volume ratio of PI is $\sim 5\%$ greater than that of An_2 . This indicates that PI is more compact than An_2 and perhaps less able to respond to pressure by undergoing conformational changes. Instead, PI may have to respond to increased pressure by undergoing a chemical reaction, consistent with our observations.

The fact that isotropic compression is able to drive the dissociation reaction is also surprising from a fundamental standpoint. Previous workers have emphasized the role of shear stress in the breaking of chemical bonds.^{2,52} There are many examples of molecules that are inert under pressure but that react when subjected to shear or a combination of shear and pressure.⁵³ Isotropic compression can drive chemical reactions, but this is a second order effect,⁵⁴ and the pressures required to break bonds are typically much higher than used in this work. Recent theoretical simulations of force-induced reactivity in isolated molecules tend to assume that the potential energy surface is distorted due to directional forces at the molecular level.^{16,55–57} Amorphous polymers are more isotropic than crystalline systems, but under compression, anisotropic forces can arise at the molecular level. Note that in the present study, the mechanochemical reaction does not directly involve the polymer host, as in previous studies of tension-induced bond breaking in polymers.^{1,58} Nevertheless, the geometry of the reaction cavity geometry can play an important role in

determining chemical reactivity,^{59,60} and the local elastic properties of the medium have been emphasized in the work Luty and Eckhardt.^{61,62} It is possible that at the molecular level, the PI molecule experiences an effective shear that can bend bonds and lead to reaction. The question then becomes what type of bond bending could lead to the observed dissociation reaction. The negative activation volume from Figure 5, as well as the lower activation energy at high pressure seen in Figure 4, both suggest that it is the transition state, rather than the equilibrium states, that is sensitive to pressure. In fact, any reaction with a negative activation volume will accelerate at higher pressures, as the pressure acts as an effective catalyst. However, in general, a negative activation volume is associated with bond formation, not breaking.⁴⁷ Therefore, it is interesting to speculate about the structure associated with the -3% volume contraction in the PI → BA transition state. The cyclobutane rings are particularly vulnerable to increases in tension across the ring. The obvious mechanism to increase this tension would be a flattening of the anthracene rings. If this occurs in a sequential manner, where the anthracene rings flatten (decreasing the butterfly angle) while the cyclobutane rings remain intact, the overall volume would temporarily decrease in the transition state. After the cyclobutane rings break, the two anthracene moieties would move apart, increasing the volume back to the original BA conformation. The initial flattening of the "butterfly" would be an example of shear force on the molecular scale. This two-step mechanism provides a plausible path by which the PI → BA reaction could proceed through a lower volume intermediate.

From this perspective, the relative insensitivity of An₂ to pressure could have several explanations. First, as discussed earlier, An₂ is not as compact as PI and may be better able to accommodate the increased density of surrounding molecules at higher pressures. An₂ would not be expected to be as constrained in its motion as PI because the lack of cyclobutane rings makes it more conformationally flexible. If the anthracene rings can shift with respect to each other in An₂, that motion can accommodate increased pressure more readily than in PI. We cannot rule out a small pressure-induced increase in the dissociation rate of An₂, but the rate remains negligible and is not observed experimentally over the pressure range investigated. The intrinsic rate is so small that even an order of magnitude enhancement would be difficult to detect on a reasonable time scale.

One last point is that the presence of the dimethyl linkers appears to be important for making a photodimer whose dissociation rate is sensitive to modest pressure increases. It has been shown that various linker modifications can change to the relative stability of the monomer and photoproduct species.^{34,35} Increasing the linker length from dimethylene to [-CH₂-N(-R)-CH₂-] and decorating the linker with R groups can lead to a thermodynamically stable dimerized state.³⁴ Similarly, the appendage of alkyl ester groups on the 9-position of anthracene lowers the photodecomposition efficiency and also stabilized the dimerized photoproduct.³⁵ The ability to characterize the role that ring strain, molecular volume, and thermodynamics play in photodimerization reactions opens the door for the design of molecular systems engineered to have enhanced mechanochemical response.

5. CONCLUSIONS

This paper has demonstrated the pressure-activated, covalent bond breaking for the photoisomer of bis-anthracene in a UV

transparent Zeonex polymer matrix. The tethered chromophores in BA provide a favorable topochemical orientation for the dimerization of the two anthracene moieties as compared to the untethered polyacenes (e.g., dianthracene, dipentacene, etc.). Thermal dissociation is largely absent for untethered dimers such as dianthracene due to high reaction barriers, and anthracene photodimers are generally regarded as stable chemical species. In contrast, we find that a modest increase in pressure results in a drastic acceleration of the PI dissociation reaction, speeding it up by almost 2 orders of magnitude. Pressure-dependent PI → BA kinetics yield a negative activation volume of -16 Å³, while temperature-dependent rate measurements at high pressure show an order of magnitude reduction in the activation energy. Taken together, these observations suggest that the pressure-induced PI → BA dissociation is a kinetic effect due to a lower volume transition state that catalyzes the reaction. At the macroscopic level, this effect is driven by isotropic compression. It is possible that the hydrostatic pressure is transformed into a locally anisotropic force, resulting in a molecular deformation that accelerates bond scission. The use of relatively mild pressures, rather than macroscopic shear, crystal fracture, or sonication, makes this a novel approach to transform mechanical forces into chemical reactivity. These results suggest that making strained molecules, possibly via photochemistry, whose transition states are sensitive to pressure, may be a fruitful approach for engineering mechanochromic systems. Current efforts are focused on making new mechanochemical architectures by altering the tethers, shifting the optical absorption to lower energies, and increasing the mechanosensitivity.

AUTHOR INFORMATION

Corresponding Author

christopher.bardeen@ucr.edu

Notes

The authors declare no competing financial interest.

ACKNOWLEDGMENTS

C.J.B. acknowledges support by the National Science Foundation, (DMR-0907310). E.L.C. acknowledges support by the ACS Petroleum Research Fund (#37400-ACS) and the National Science Foundation (CHE-0612957). Prof. Gregory Beran is acknowledged for his help with D-DFT calculations.

REFERENCES

- (1) Beyer, M. K.; Clausen-Schaumann, H. *Chem. Rev.* **2005**, *105*, 2921.
- (2) Todres, Z. V. *Organic Mechanochemistry and Its Practical Applications*; CRC Press: Boca Raton, FL, 2006.
- (3) Kaupp, G. *CrystEngComm* **2009**, *11*, 388.
- (4) Mori, Y.; Yamada, N.; Kanazawa, M.; Horikoshi, Y.; Watanabe, Y.; Maeda, K. *Bull. Chem. Soc. Jpn.* **1996**, *69*, 2355.
- (5) Sheth, A. R.; Lubach, J. W.; Munson, E. J.; Muller, F. X.; Grant, D. J. W. *J. Am. Chem. Soc.* **2005**, *127*, 6641.
- (6) Ito, H.; Saito, T.; Oshima, N.; Kitamura, N.; Ishizaka, S.; Hinatsu, Y.; Wakeshima, M.; Kato, M.; Tsuge, K.; Sawamura, M. *J. Am. Chem. Soc.* **2008**, *130*, 10044.
- (7) Zhang, G.; Lu, J.; Sabat, M.; Fraser, C. L. *J. Am. Chem. Soc.* **2010**, *132*, 2160.
- (8) Davis, D. A.; Hamilton, A.; Yang, J.; Cremer, L. D.; Gough, D. V.; Potisek, S. L.; Ong, M. T.; Braun, P. V.; Martinez, T. J.; White, S. R.; Moore, J. S.; Sottos, N. R. *Nature* **2009**, *459*, 68.
- (9) Lenhardt, J. M.; Ong, M. T.; Choe, R.; Evenhuis, C. R.; Martinez, T. J.; Craig, S. L. *Science* **2010**, *329*, 1057.

- (10) Wu, D.; Lenhardt, J. M.; Black, A. L.; Akhremitchev, B. B.; Craig, S. L. *J. Am. Chem. Soc.* **2010**, *132*, 15936.
- (11) Hickenboth, C. R.; Moore, J. S.; White, S. R.; Sottos, N. R.; Baudry, J.; Wilson, S. R. *Nature* **2007**, *446*, 423.
- (12) Klukovich, H. M.; Kean, Z. S.; Iacono, S. T.; Craig, S. L. *J. Am. Chem. Soc.* **2011**, *133*, 17882.
- (13) Karthikeyan, S.; Sijbesma, R. P. *Nature Chem.* **2010**, *2*, 436.
- (14) Basedow, A. M.; Ebert, K. H. *Adv. Polym. Sci.* **1977**, *22*, 83.
- (15) Wiggins, K. M.; Hudnall, T. W.; Shen, Q. L.; Kryger, M. J.; Moore, J. S.; Bielawski, C. W. *J. Am. Chem. Soc.* **2010**, *132*, 3256.
- (16) Ribas-Arino, J.; Shiga, M.; Marx, D. *J. Am. Chem. Soc.* **2010**, *132*, 10609.
- (17) Kryger, M. J.; Munaretto, A. M.; Moore, J. S. *J. Am. Chem. Soc.* **2011**, *133*, 18992.
- (18) Nguyen, T. Q.; Kausch, H. H. *Adv. Polym. Sci.* **1992**, *100*, 73.
- (19) Fanselow, D. L.; Drickamer, H. G. *J. Chem. Phys.* **1974**, *61*, 4567.
- (20) Wilson, D. G.; Drickamer, H. G. *J. Chem. Phys.* **1975**, *63*, 3649.
- (21) Kawamura, I.; Degawa, Y.; Yamaguchi, S.; Nishimura, K.; Tuzi, S.; Saito, H.; Naito, A. *Photochem. Photobiol.* **2007**, *83*, 346.
- (22) Tabata, M.; Tanaka, Y.; Sadahiro, Y.; Sone, T.; Yokota, K.; Miura, I. *Macromolecules* **1997**, *30*, 5200.
- (23) Sakashita, M.; Yamakawa, H.; Fujihisa, H.; Aoki, K.; Sasaki, S.; Shiimizu, H. *Phys. Rev. Lett.* **1997**, *79*, 1082.
- (24) Benedetti, L. R.; Nguyen, J. H.; Caldwell, W. A.; Liu, H.; Kruger, M.; Jeanloz, R. *Science* **1999**, *286*, 100.
- (25) Zeng, Q.; He, Z.; San, X.; Ma, Y.; Tian, F.; Cui, T.; Liu, B.; Zou, G.; Mao, H. *Proc. Nat. Acad. Sci.* **2008**, *105*, 4999.
- (26) Splitter, J. S.; Calvin, M. *J. Org. Chem.* **1958**, *23*, 651.
- (27) Irie, M. *Chem. Rev.* **2000**, *100*, 1685.
- (28) Jones, G.; Reinhardt, T. E.; Bergmark, W. R. *Sol. Energy* **1978**, *20*, 241.
- (29) Al-Kaysi, R. O.; Bardeen, C. J. *Adv. Mater.* **2007**, *19*, 1276.
- (30) Al-Kaysi, R. O.; Muller, A. M.; Bardeen, C. J. *J. Am. Chem. Soc.* **2006**, *128*, 15938.
- (31) Zhu, L.; Agarwal, A.; Lai, J.; Al-Kaysi, R. O.; Tham, F. S.; Ghaddar, T.; Mueller, L.; Bardeen, C. J. *J. Mater. Chem.* **2011**, *21*, 6258.
- (32) Zhu, L.; Al-Kaysi, R. O.; Bardeen, C. J. *J. Am. Chem. Soc.* **2011**, *133*, 12569.
- (33) Zhu, L.; Al-Kaysi, R. O.; Dillon, R. J.; Tham, F. S.; Bardeen, C. J. *Cryst. Growth Des.* **2011**, *11*, 4975.
- (34) Usui, M.; Shindo, Y.; Nishiwaki, T.; Anda, K.; Hida, M. *Chem. Lett.* **1990**, 419.
- (35) Salt, K.; Scott, G. W. *J. Phys. Chem.* **1994**, *98*, 9986.
- (36) Berg, O.; Chronister, E. L.; Yamashita, T.; Scott, G. W.; Sweet, R. M.; Calabrese, J. *J. Phys. Chem. A* **1999**, *103*, 2451.
- (37) Golden, J. H. *J. Chem. Soc.* **1961**, 3741.
- (38) Zhu, A.; Wang, B.; White, J. O.; Drickamer, H. G. *J. Phys. Chem. A* **2003**, *107*, 6932.
- (39) Peverati, R.; Baldrige, K. K. *J. Chem. Theory Comput.* **2009**, *5*, 2772.
- (40) Bao, D.; Ramu, S.; Contreras, A.; Upadhyayula, S.; Vasquez, J. M.; Beran, G.; Vullev, V. I. *J. Phys. Chem. B* **2010**, *114*, 14467.
- (41) Birks, J. B. *Photophysics of Aromatic Molecules*; Wiley-Interscience: New York, 1970.
- (42) Mau, A. W. H. *J. Chem. Soc.-Faraday Trans. I* **1978**, *74*, 603.
- (43) Greene, F. D. *Bull. Soc. Chim. France* **1960**, 1356.
- (44) Ehrenber, M. *Acta Crystallogr.* **1966**, *20*, 182.
- (45) Dunand, A.; Ferguson, J.; Puza, M.; Robertson, G. B. *Chem. Phys.* **1980**, *53*, 225.
- (46) Wada, A.; Tanaka, J. *Acta Crystallogr., Sect. B: Struct. Sci.* **1977**, *33*, 355.
- (47) Luft, G.; Recasens, F.; Velo, E. *High Pressure Process Technology: Fundamentals and Applications*; Bertuccio, A., Vetter, G., Eds.; Elsevier: Amsterdam, 2001; Vol. 9, pp 65–140.
- (48) Trzop, E.; Turowska-Tyrk, I. *Acta Crystallogr., Sect. B: Struct. Sci.* **2008**, *64*, 375.
- (49) Choi, C. S.; Marinkas, P. L. *Acta Crystallogr., Sect. B: Struct. Sci.* **1980**, *36*, 2491.
- (50) Hamann, S. D.; Linton, M.; Sasse, W. H. F. *Aust. J. Chem.* **1980**, *33*, 1419.
- (51) Julian, M. M. *Acta Crystallogr., Sect. A* **1973**, *A 29*, 116.
- (52) Gilman, J. J. *Science* **1996**, *274*, 65.
- (53) Bridgman, P. W. *Phys. Rev.* **1935**, *48*, 825.
- (54) Gilman, J. J. In *Metal-Insulator Transitions Revisited*; Edwards, P. P., Rao, C. N. R., Eds.; Taylor & Francis: London, 1995; p 269.
- (55) Dopieralski, P.; Ribas-Arino, J.; Marx, D. *Angew. Chem., Int. Ed.* **2011**, *50*, 7105.
- (56) Bailey, A.; Mosey, N. J. *J. Chem. Phys.* **2012**, *136*, 044102/1.
- (57) Konda, S. S. M.; Brantley, J. N.; Bielawski, C. W.; Makarov, D. E. *J. Chem. Phys.* **2011**, *135*, 164103/1.
- (58) Caruso, M. M.; Davis, D. A.; Shen, Q.; Odom, S. A.; Sottos, N. R.; White, S. R.; Moore, J. S. *Chem. Rev.* **2009**, *109*, 5755.
- (59) Cohen, M. D. *Angew. Chem., Int. Ed.* **1975**, *14*, 386.
- (60) McBride, J. M.; Segmuller, B. E.; Hollingsworth, M. D.; Mills, D. E.; Weber, B. A. *Science* **1986**, *234*, 830.
- (61) Luty, T.; Eckhardt, C. J. *J. Am. Chem. Soc.* **1995**, *117*, 2441.
- (62) Luty, T.; Ordon, P.; Eckhardt, C. J. *J. Chem. Phys.* **2002**, *117*, 1775.